Unified Direct-Flux Vector Control for AC Motor Drives

Unified Direct-Flux Vector Control for AC Motor Drives

G. Pellegrino
Member, IEEE
gianmario.pellegrino@polito.it

R. Bojoi
Senior Member, IEEE
radu.bojoi@polito.it

P. Guglielmi
Member, IEEE
paolo.guglielmi@polito.it

Politecnico di Torino, Corso Duca degli Abruzzi 24, Torino, 10129 Italy

Abstract -- **The paper introduces a Unified Direct-Flux Vector Control scheme suitable for sinusoidal AC motor drives. The AC drives considered here are Induction Motor, Synchronous Reluctance and synchronous Permanent Magnet motor drives, including Interior and Surface-mounted Permanent Magnet types. The proposed controller operates in stator flux coordinates: the stator flux amplitude is directly controlled by the direct voltage component, while the torque is controlled by regulating the quadrature current component. The unified direct-flux control is particularly convenient when flux-weakening is required, since it easily guarantees maximum torque production under current and voltage limitations. The hardware for control is standard and the control firmware is the same for all the motors under test with the only exception of the magnetic model used for flux estimation at low speed. Experimental results on four different drives are provided, showing the validity of the proposed unified control approach.**

Index Terms -- Variable Speed Drives, Synchronous Motor Drives, Permanent magnet machines, Traction Motor Drives, Motion Control, Flux-weakening, Limited Voltage Control.

I. INTRODUCTION

The concept of a unified control scheme to be used with different AC motors is known from more than one decade: industrial controllers are available on the market [1] and unified vector control schemes have been proposed in the literature for Induction Motor (IM) and Surface-mounted Permanet Magnet (SPM) motor drives [2]. The general approach called "active-flux" proposed in [3] covered IM and SPM as well as Interior Permanent-Magnet (IPM), Synchronous Reluctance (SyR) and wound rotor synchronous motors. All the cited schemes [1-3] use rotor flux orientation and current vector control. A different approach, based on direct flux, direct torque control has been also proposed as UNIDRIVE in [4].

The goal of the paper is to propose a control strategy with high degree of generality to be used either with IM, IPM, SPM and SyR motor drives. Respect to other unified solutions based on rotor flux (or active flux) orientation, the proposed Unified Direct-Flux Vector Control (UDFVC) scheme uses a Direct Stator Flux Control (DSFC) approach implemented in the stator flux reference frame. The stator flux is directly controlled by the *d*-axis component of the stator voltage vector, while the torque is controlled by regulating the *q*-axis component of the stator current vector. The direct flux control makes the proposed UDFVC very effective in terms of voltage utilization in the flux-weakening region, that is particularly used in traction, spindle drives and home appliances. For all the motor types the inverter voltage and current limits are fully exploited in flux-weakening with no need of knowledge of the motor model (except for the stator resistance), even in the case of a variable DC link voltage [5-6].

The motor magnetic model (or current model) is used for flux estimation at low speed as for most IM field-oriented control schemes [7] and as it is also usual for position sensorless control techniques [8]. Eventual parameter errors can lead to a flux estimation error in the low speed region, and to a possible steady-state torque estimation error. However, the control is robust in all the speed range and its dynamic response is independent of the model errors.

In this paper, only sensored operation is addressed, i.e. the rotor position is measured by means of a position sensor. However, the unified control can be easily extended to sensorless applications, as already shown for the IM [6]. Experimental results are presented for IM, IPM, SPM and SyR machines, showing the feasibility of the proposed control, and in particular the robust flux-weakening operation.

II. AC MACHINES MODELING

As a general notation, the machine stator vectors (voltage, flux, current) will be called $\bar{v}$, $\bar{\lambda}$ and $\bar{i}$ respectively, and the subscript "*s*" will refer to the stator flux reference frame when associated to those variables. The adopted vector reference frames are defined in Fig. 1, for all the considered machines: stationary frame (α,β), rotor frame (d_m,q_m), rotor flux frame (d,q) and stator flux frame (d_s,q_s). For convenience, <u>*the axis alignment chosen for the SyR motor (Fig. 1-d) is unconventional*</u>, with the *d*-axis along the minimum permeance direction instead of the maximum permeance one as more usual in the literature. This choice permits to adopt unified magnetic equations for the three synchronous machines (SyR, IPM, SPM), as clarified in the following.

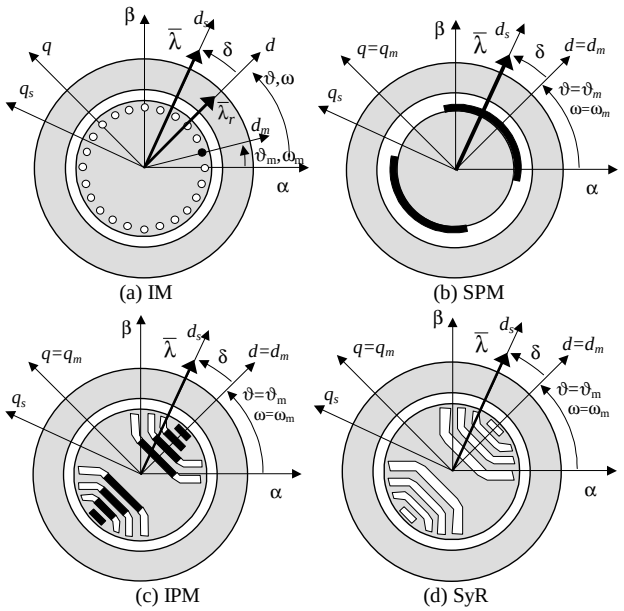

Figure 1. Definiton of common reference frames for all AC machines.

Independently of the adopted reference frame (stationary, rotor flux, stator flux), all the considered AC machines have the same voltage model and torque expressions. For example, in the rotor synchronous frame we get:

$$\bar{v}_{dq} = R_s \cdot \bar{i}_{dq} + \frac{d\bar{\lambda}_{dq}}{dt} + j\omega\bar{\lambda}_{dq} \tag{1}$$

$$T = \frac{3}{2} \cdot p \cdot \left(\lambda_d i_q - \lambda_q i_d\right) \tag{2}$$

where R_s is the stator resistance, ω is the synchronous speed and p is the number of pole-pairs.

Each machine has its own specific current-to-flux vector relationship: in the following subsections, the magnetic models of the considered motors will be briefly summarized, expressed in the rotor mechanical frame (d_m,q_m) that coincides with the rotor synchronous frame (d,q) for all the synchronous machines. The reason of this choice will be better clarified in the "Stator flux observer" subsection (IV.A).

A. IPM, SyR and SPM motor magnetic models

The simplified IPM magnetic model in rotor coordinates can be expressed as

$$\bar{\lambda}_{dq} = \begin{bmatrix} L_d & 0 \\ 0 & L_q \end{bmatrix} \cdot \bar{i}_{dq} + \begin{bmatrix} \lambda_m \\ 0 \end{bmatrix} \tag{3}$$

where L_d and L_q are the d-axis and q-axis inductances and λ_m is the PM linked flux or no-load flux linkage.

The model of an isotropic SPM motor is also represented by (3), with $L_d = L_q = L_s$, while the model of a SyR motor is (3) with $\lambda_m = 0$.

A more realistic model should account for magnetic saturation and cross-saturation [9], in particular for IPM and SyR motors. As shown in the following, the model accuracy has an effect only at very low speed. To get an accurate torque estimation around zero speed, the magnetic model should be accurate and implemented in the form of 2-dimensional look-up tables $\lambda_d(i_d, i_q)$ and $\lambda_q(i_d, i_q)$ as suggested in [10], otherwise simplified models are working well.

B. IM magnetic model

The current to flux relationship for the IM is (4), where the rotor flux can be derived from the rotor equation (5) [7].

$$\bar{\lambda} = k_r \cdot \bar{\lambda}_r + \sigma L_s \cdot \bar{i} \tag{4}$$

$$\tau_r \frac{d\bar{\lambda}_{r,dqm}}{dt} + \bar{\lambda}_{r,dqm} = L_m \cdot \bar{i}_{dqm} \tag{5}$$

where σ is the leakage factor, L_s is the stator inductance, $\tau_r = L_r/R_r$ is the rotor time constant and $k_r = L_m/L_r$ is the rotor coupling factor. As said, the rotor reference frame (d_m,q_m) has been adopted in (5).

III. Unified Direct-Flux Vector Control in Stator Flux Coordinates

The voltage model (6) and torque equation (7) are common to all the machines also <u>*in the stator flux frame*</u> as

$$\bar{v}_{dqs} = R_s \cdot \bar{i}_{dqs} + \frac{d}{dt} \cdot \begin{bmatrix} \lambda \\ 0 \end{bmatrix} + \lambda \cdot \begin{bmatrix} 0 \\ \omega + \frac{d\delta}{dt} \end{bmatrix} \tag{6}$$

$$T = \frac{3}{2} \cdot p \cdot \lambda \cdot i_{qs} \tag{7}$$

where δ is the *load angle*, i.e. the phase angle of the stator flux with respect to the rotor flux (IM) or with respect to the d-axis (SyR, SPM, IPM).

From (6) it results that the stator flux amplitude λ can be regulated by means of the d_s-axis voltage and the load angle (i.e. torque) by means of the q_s-axis voltage. However, the unified torque expression (7) suggests that the control of the q_s-axis current instead of the load angle may lead to a simple and unified torque control scheme [5-6]. For this reason, a further manipulation of the quadrature state equation in (6) is necessary for all the machines.

A. Quadrature current equation for IPM, SyR and SPM

As described in [5], the q_s-axis current equation for an IPM motor is

$$L_d \frac{di_{qs}}{dt} = -R_s i_{qs} + k \cdot \left(v_{ds} - R_s \cdot i_{ds}\right) + b \cdot \left(v_{qs} - \omega \cdot \lambda\right) \tag{8}$$

where the two factors k and b are defined in (9) for the IPM, in (10) for the SyR and in (11) for the SPM.

$$\begin{cases} k_{IPM}(\delta) = \frac{1}{2} \cdot \left(1 - \frac{L_d}{L_q}\right) \cdot sin(2\delta) \\ b_{IPM}(\lambda,\delta) = -\left(1 - \frac{L_d}{L_q}\right) \cdot cos(2\delta) + \frac{\lambda_m}{\lambda} \cdot cos(\delta) \end{cases} \tag{9}$$

For the SyR motor the k factor is the same of (9), while the b factor is obtained by posing λ_m equal to zero:

$$\begin{cases} k_{SyR}(\delta) = k_{IPM}(\delta) \\ b_{SyR}(\lambda,\delta) = -\left(1 - \dfrac{L_d}{L_q}\right)\cdot\cos(2\delta) \end{cases} \quad (10)$$

The SPM motor has k equal to zero and a simplified expression of b:

$$\begin{cases} k_{SPM} = 0 \\ b_{SPM}(\lambda,\delta) = \dfrac{\lambda_m}{\lambda}\cdot\cos(\delta) \end{cases} \quad (11)$$

It must be underlined that the b factor is representative of the torque derivative with respect to the load angle δ, as addressed in [5].

$$b = \frac{L_d}{\lambda^2}\cdot\left.\frac{\partial T}{\partial\delta}\right|_{\lambda=const} \quad (12)$$

The effects of b in flux-weakening operation, and in particular the relationship between b and the Maximum Torque per Voltage (MTPV) operation will be put in evidence in the following (III.C – III.E).

B. *Quadrature current equation for IM*

As shown in [6], the q_s-axis current equation for an IM is:

$$\sigma L_s \frac{di_{qs}}{dt} = -R_{eq}\cdot i_{qs} - \omega_{slip}\cdot\sigma L_s\cdot i_{ds} + \left(v_{qs} - \omega_m\cdot\lambda\right) \quad (13)$$

where $R_{eq} = R_s + k_r/k_s \cdot R_r$ and ω_{slip} is the slip speed defined as $\omega_{slip} = \omega - \omega_m$.

C. *Direct flux vector control*

From the machine models (6-13), it follows that:

a) The stator flux regulation by means of the d_s voltage is decoupled from the q_s axis and leads to a closed-loop bandwidth that is directly imposed by the proportional gain of a proportional-integral (PI) flux controller with no influence of magnetic saturation.

b) The torque can be regulated by controlling the q_s current component via the q_s-axis voltage using a PI current controller. The bandwidth of the q_s-axis current loop is imposed by the proportional gain of the PI current controller and the inductance L_q (IPM and SyR), σL_s (IM) or L_s (SPM).

c) For all motors save the SPM (that has $k_{SPM} = 0$) the control of i_{qs} (torque) is dynamically coupled with the flux control axis. This is usual with Stator Field Oriented Control (SFOC) of IMs. The advantages and disadvantages of SFOC with respect to rotor field oriented control have been comprehensively analyzed for IM [11], showing that the torque dynamics can be made comparable with proper compensation [12]. It must be also considered that IPM and SyR motors would have shown a *d-q* coupling also if the rotor reference frame was adopted, since both (d,q) current components give torque contributions.

d) All the synchronous motors (SPM, IPM, SyR) have to cope with the variable b term in (8). Once the bandwidth of q_s-axis current regulation is imposed by a proper design of PI current controller, the torque response depends on the b value. This means that: 1) at rated torque (low speed and rated flux and load angle) the torque response is very fast, being similar with the torque response obtained by current-controlled AC drives using (d,q) rotor flux frame and 2) at high speed (during flux-weakening) the torque response can become slower since b is reduced, but it is unlikely that step torque disturbances are applied at such high speeds.

e) For IPM and SyR motors, the coupling of the i_{qs} equation with the direct axis, i.e. the effect of the v_{ds} voltage component on the i_{qs} dynamics depends on the term $k(\delta)$ in (9) and (10) respectively and is visible during flux regulation transients only (at steady state $v_{ds} = R_s \cdot i_{ds}$). The closed-loop control of i_{qs} rejects the effects of such moderate cross-coupling. Model-based compensation is also possible in case of severe dynamics requirements.

f) For IMs, equation (13) shows two coupling terms, i.e. $\lambda\cdot\omega_m$ and $\sigma L_s\cdot\omega_{slip}\cdot i_{ds}$. Both terms can be estimated and compensated in a feedforward fashion. The first term is not critical for torque dynamics since it is slowly varying during flux regulation or speed variations. The second term requires the estimation of the slip speed, as in [12].

g) The (λ, i_{qs}) control is stable for torque values under the pull-out torque limit, also called maximum torque per flux or Maximum Torque per Voltage (MTPV) limit. This is particularly evident from (8, 9) for the synchronous machines. The i_{qs} control loop is stable if $b(\lambda,\delta)>0$, while it becomes unstable if $b < 0$, according to (8). It will be shown in the following that the $b = 0$ boundary coincides with the MTPV trajectory. MTPV operation is achieved in the proposed control by limiting the flux phase angle δ to be under a proper maximum value that is typical of each motor type.

D. *Maximum torque per voltage operation*

The MTPV operation occurs in the flux-weakening region at high speed and it is also called *voltage limited operation* [13]. Given the voltage limit, over a certain speed it is no longer convenient to exploit the full inverter current I_{max} for obtaining the maximum machine torque, because the pull-out torque limit has been reached. The pull-out torque condition coincides with a specific value of the load angle δ. Such value will be indicated as δ_{max} from now on and varies with the motor type. Below the pull-out limit the flux phase angle is $\delta < \delta_{max}$. The expression of δ_{max} for the considered motors is obtained by expressing the electromagnetic torque (2) as a function of the flux amplitude and phase, and then posing to zero the torque partial derivative with respect to δ, that is at constant flux amplitude.

E. *Pull out torque angle of IPM, SyR and SPM motors*

The manipulation of (2) and (3) leads to

$$T = \tfrac{3}{2} \cdot \frac{p}{L_d} \cdot \left(-\frac{L_q - L_d}{L_q} \cdot \lambda^2 \cdot \frac{\sin 2\delta}{2} + \lambda_m \lambda \sin\delta \right) \quad (14)$$

The torque derivative with respect to δ is

$$\frac{\partial T}{\partial \delta} = \tfrac{3}{2} \cdot \frac{p}{L_d} \cdot \left(-\frac{L_q - L_d}{L_q} \cdot \lambda^2 \cdot \cos 2\delta + \lambda_m \lambda \cos\delta \right) \quad (15)$$

By imposing (15) to be equal to zero, the MTPV load angle condition is obtained as

$$\frac{L_q - L_d}{L_q} \cdot \lambda^2 \cdot \cos 2\delta = \lambda_m \lambda \cos\delta \quad (16)$$

For the SyR and SPM motors, eq. (16) has an easy solution. In particular, for SyR motor the right side of (16) is zero ($\lambda_m = 0$) and leads to

$$\delta_{max,SyR} = 135° \quad (17)$$

For SPM the left side of (16) is zero ($L_d = L_q$), i.e.

$$\delta_{max,SPM} = 90° \quad (18)$$

A comment is needed about the SyR motor. The value 135° has been obtained here because of the particular choice of the reference axes, introduced in Fig. 1 and commented in section II. With the adopted axes, the motoring operation of the SyR machine is in the second quadrant of the *dq* plane, thus the 135° value is the corrected value to be considered. With standard (*d,q)* axes the more familiar solution $\delta_{max} = 45°$ (first quadrant) would have been obtained for motoring.

Dealing with the IPM motor, the solution of (16) depends of the relationship between the motor saliency, represented by the $(L_q - L_d)/L_q$ term, and the PM flux, both being dependent on the motor design. In any case, the solution of (16) leads to a δ_{max} that is an intermediate value between the values given in (17) and (18):

$$90° < \delta_{max,IPM} < 135° \quad (19)$$

For IPM motors with high saliency, the value approaches 135° as for a SyR motor, while it moves towards 90° for low saliency motors, as for an SPM motor.

According to the definition of *b* given by (12), the condition $b = 0$ coincides with the MTPV operation. As said, the i_{qs} control would become instable in case of $b < 0$, thus the correct exploitation of the MTPV control trajectory maintains the proposed control stable over the whole speed range, as it will be shown in sections IV and V.

F. Pull out torque angle of the IM

In rotor flux coordinates, the substitution of $\lambda_r = L_m\, i_d$ in (4) leads to

$$\bar{\lambda}_{dq} = \begin{bmatrix} L_s & 0 \\ 0 & \sigma L_s \end{bmatrix} \cdot \bar{i}_{dq} \quad (20)$$

From (2) and (20) the torque expression becomes

$$T = \tfrac{3}{2}\, p \cdot \frac{1-\sigma}{\sigma L_s} \cdot \lambda^2 \cdot \frac{\sin 2\delta}{2} \quad (21)$$

The torque derivative with respect to δ is

$$\frac{\partial T}{\partial \delta} = \tfrac{3}{2}\, p \cdot \frac{1-\sigma}{\sigma L_s} \cdot \lambda^2 \cdot \cos 2\delta \quad (22)$$

The MTPV load angle is obtained when (22) is zero, i.e.

$$\delta_{max,IM} = 45° \quad (23)$$

IV. UDFVC IMPLEMENTATION

The proposed UDFVC control scheme is shown in Fig. 2 for a speed-controlled AC drive. The flux and quadrature current references (λ^*, i_{qs}^*) are computed from the torque reference using (7). The flux set-point at low speed can be either a constant value (e.g. for IM and SyR drives) or a function of the torque set-point. In Fig. 2 the Maximum Torque per Ampere (MTPA) law has been chosen, but simpler functions are possible with no significant side-effects [5]. The main blocks of Fig. 2 are discussed in the following subsections.

A. Stator flux observer

The unified stator flux observer (Fig. 3) is based on the current-to-flux model at low speed and on back-EMF integration at high speed [7,14]. The magnetic model is represented for all the machines in the (d_m,q_m) rotor frame (see Section II). In general terms, such scheme can be indicated as a reduced-order $VI\theta_m$ closed-loop observer. The crossover angular frequency ω_{co} between low-speed and high speed models coincides with the observer gain *g* (rad/s).

As said, for synchronous machines the simple magnetic model (3) or more accurate models can be adopted. For IM drives the model is (5) and it is affected, as usual, by the uncertainty on the parameters L_m and τ_r. In case of an inaccurate model, the obtained torque differs from the torque set point but the control is still stable. In other words, <u>*the motor parameter inaccuracies or variations affect only the drive performance at low-speed*</u> and not the high-speed operation, as it happens with pure current vector control where the flux weakening trajectories are based on the model.

The observer outputs needed for control are evidenced in Fig. 3. In particular, the sine and cosine of the flux phase angle $\theta + \delta$ are obtained dividing the α, β flux components by the flux amplitude. Moreover, the sine and cosine of the load angle δ are obtained by a further coordinate rotation: the angle θ coincides with θ_m for the synchronous machines, while for the IM case it is the phase angle of the rotor flux vector (Fig. 1a) and its sine and cosine (needed for the coordinate rotation of Fig. 3) are estimated using (4) for rotor flux estimation. In those applications where very low speed operation is not required and/or the starting torque is moderate, the magnetic model feedback can even become unnecessary.

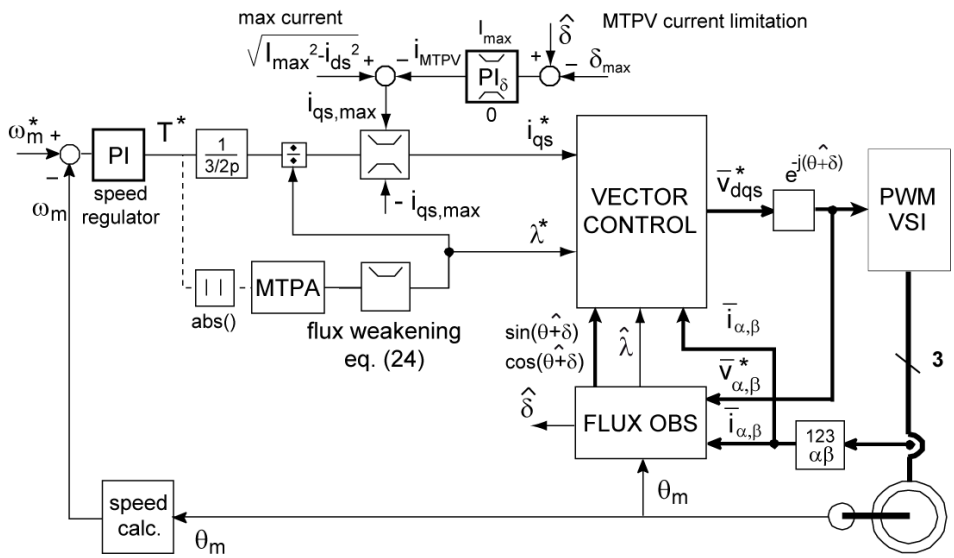

Figure 2. Unified direct-flux vector control scheme.

The observer scheme of Fig. 3 can be simplified in the form of a simple stator flux estimator with Low-Pass Filter (LPF), where the gain g is the LPF pole [15]. Gain and phase compensation may be required, depending on g value and the minimum electrical speed ω.

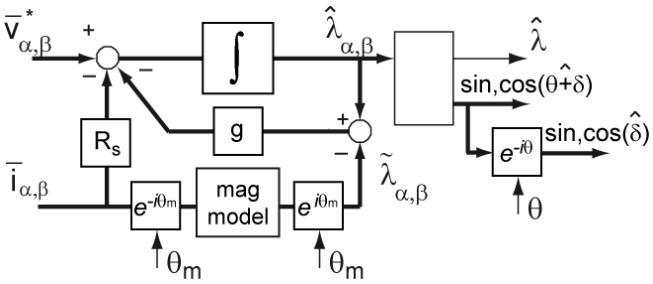

Figure 3. Unified $VI\theta_m$ flux observer. The the angle θ is θ_m for the synchronous motors whilst it is the rotor flux position for the IM, estimated by means of (4) applied to the observed stator flux.

B. Vector control

The vector control block in Fig. 2 contains the flux and quadrature current regulators that give the voltage reference in stator flux coordinates. The flux and current controllers are simple PI regulators and the firmware is the same for all the motors. The bandwidth of the λ control is independent of magnetic saturation and machine model, thus <u>*the settings of the PI flux regulator are the same for all the motors*</u>. The i_{qs} control loop, according to (8), has disturbance terms. The term $\omega_m\lambda$ is feed-forward compensated in all the motors, while the other terms are compensated by the integrative action of the current controller.

C. Maximum voltage limitation

The maximum voltage limit is respected by limiting the flux reference according to the synchronous speed and the actual DC link voltage (24).

$$\lambda^* \le \left[V_{max} - R_s \cdot i_{qs} \cdot sign(\omega)\right] / |\omega| \qquad (24)$$

where V_{max} is the inverter maximum voltage that is updated according to the measured DC link voltage [5-6]. The setting of V_{max} determines whether the inverter overmodulation region is exploited or not. A typical setting uses $V_{max} = v_{dc}/\sqrt{3}$, where v_{dc} is the measured DC link voltage. The resistive term in (24) is used only for low power motors, otherwise it can be neglected.

D. Maximum current limitation

The motor phase current is limited by saturating the quadrature current reference according to (25), where I_{max} is the inverter maximum current.

$$i_{qs}^* \le \sqrt{I_{max}^2 - i_{ds}^2} \qquad (25)$$

E. Maximum torque per voltage (MTPV) current limitation

As introduced in III.D-III.F, the MTPV operation can be obtained by limiting the load angle to be under δ_{max}, that depends of the motor type.

There is a tight relationship between the i_{qs} current component and the load angle δ. In particular, the limitation of the i_{qs} current produces a limitation of the load angle. For this reason, the MTPV operation is obtained by limiting the i_{qs} current reference, according to the observed load angle. While the just described I_{max} saturation keeps the current inside the inverter limit, this further i_{qs} limitation is performed by the same saturation block (see Fig. 2) and represented by the current component i_{MTPV}. This component, subtracted from the I_{max} limit (25), leads to a reduction of the current amplitude below the inverter maximum rating ($|i| < I_{max}$), as

requested under the pull-out torque conditions. The δ_{max} angle limits have been calculated in (17-19) and (23). Dealing with the IPM case (19), the exact value depends on the motor and can be evaluated by model manipulation or by dedicated tests at no-load with trial and error values in the range (19).

The unified calculation of the MTPV-limiting current component i_{MTPV} based on a PI controller, as shown in Fig. 2, whose output is non zero only in case the estimated load angle overcomes the set point δ_{max}. The unified estimation of the load angle error ($\delta-\delta_{max}$), that is the input of the PI regulator, requires a specific implementation. First of all, the sine and cosine components of the load angle are obtained by coordinate rotation as indicated in Fig. 3. Then, two solutions are possible: to evaluate δ as the arc tangent of its sine divided by cosine, or, to avoid the division, to evaluate $\delta-\delta_{max}$ as the cross product between the sine and cosine components of the respective angles.

The tuning of the PI regulator gains and the bandwidth of the δ_{max} limitation can be evaluated according to the simplified block scheme of Fig. 4. The inverter and flux observer dynamics have been neglected. The closed loop bandwidth of the δ_{max} limitation is:

$$\omega_{b,\delta} = \frac{k_{p,\delta} \cdot k_{p,iqs}}{\lambda} \tag{26}$$

Where $k_{p,\delta}$ and $k_{p,iqs}$ are the proportional gains of the δ_{max} and i_{qs} regulators respectively. The bandwidth depends on the flux amplitude and must be set according to its minimum value that is at maximum speed. It can be demonstrated that the PI-based δ_{max} control overcomes the instability problems of (λ, i_{qs}) control with any δ_{max} set-point, properly or improperly selected.

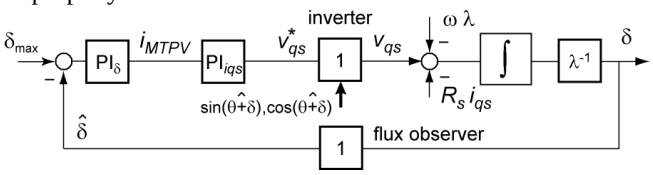

Figure 4. Dynamic block scheme representing δ_{max} regulation.

V. EXPERIMENTAL RESULTS

Experimental tests have been carried out on four different machines (IM, IPM, SPM, SyR), whose characteristics are reported in the Appendix.

A. Experimental setup

The IM, IPM and SyR have similar size and operating speed, according to their common application field that is home appliances. In particular, the SyR motor is derived from an IPM prototype for home appliances, assembled with no magnets for research purposes and performance comparison. Thus the SyR has a limited constant power speed range and operating speed range (0÷6000 rpm), with respect to the IM and IPM ones (0÷16000 rpm). The SPM motor is of a larger size, larger current and has a maximum speed of 6000 rpm.

Two different experimental rigs have been used for the tests. For the small size motors (IM, IPM and SyR) the inverter is rated 10A (pk) output current, with 220V/50Hz single phase AC input and passive rectifier. The controller is a dSPACE DS1103 PPC board. For the SPM motor an inverter of larger size has been used, controlled by a floating-point micro controller (ADSP 21060). The current limit is 20A in this case that is nearly half of the motor characteristic current and corresponds to a maximum speed of 6000 rpm that is the motor rating due to centrifugal constraints. The three phase currents and the dc-link voltage and rotor position are measured at a sampling frequency of 10 kHz that is also the PWM switching frequency. The position is measured by a standard incremental encoder with 512 pulses per revolution.

B. Speed reversals with deep flux-weakening operation

Results for step speed reversal are shown in Figs. 4-7 for the four machines. The reported signals are the measured speed, the controlled variables (λ, i_{qs}), one phase current and the estimated load angle. The IM speed reversal (±16000 rpm) is shown in Fig. 5: the inverter current limit is set to 8 A pk. In the low speed range (0.1s to 0.4 s), the phase currents are clamped to 8 A by the current limitation block. At high speed, the current amplitude is reduced by the MTPV i_{qs} saturation block. The deceleration (-16000 - 0 rpm) is faster than the acceleration for two reasons: (a) the motor losses (iron, copper) help braking; (b) the available voltage is higher (the regeneration charges the DC link capacitor up to the trip level of a braking resistor) and a higher flux reference is set, according to (24), from which the higher torque. The noise on i_{qs} during acceleration (Fig. 5) is due to the 100 Hz dc-link voltage ripple since the inverter is fed by a single-phase diode rectifier with 50Hz ac supply.

In Fig. 6, the speed reversal of the IPM motor has similar characteristics. The maximum current is set to 5 A pk. For most of the time the phase current amplitude is less than 5A to the MTPV limitation, while maximum current operation is evidenced at low speed (< 4000rpm).

The SyR motor speed reversal (± 6000 rpm) is shown in Fig. 7 with the current limit set to 5A pk. The motor torque is heavily MTPV limited above 4000 rpm (positive or negative) and results in a very limited speed range in flux weakening.

However, the limited speed range in flux weakening is a characteristic of the SyR motor type and not a limitation imposed by the control.

The SPM motor speed reversal (± 6000 rpm) is shown in Fig. 8 using two different ramps. The inverter current limit has been set at 20A pk. The fast ramp (top) shows that the current needed for de-magnetization at 6000rpm, no-load, is much higher than the i_{qs} current needed for fast acceleration (10A).

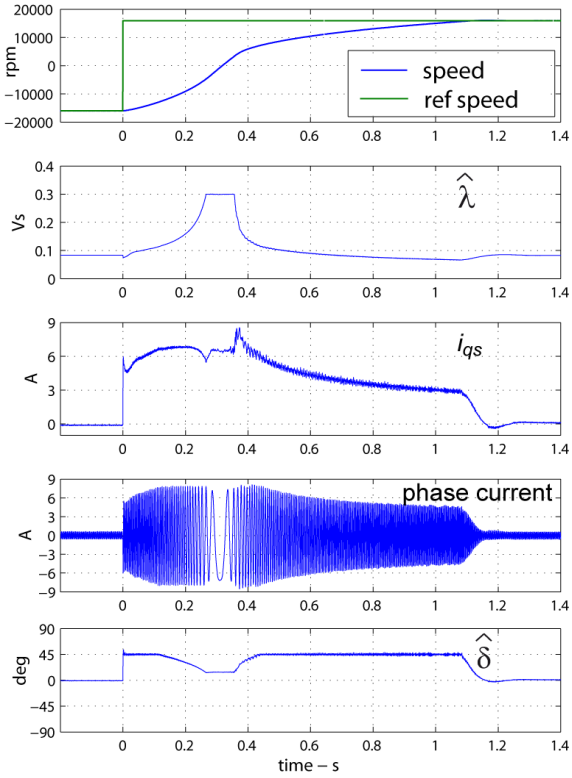

Figure 5. IM speed reversal (–16000rpm÷16000rpm).

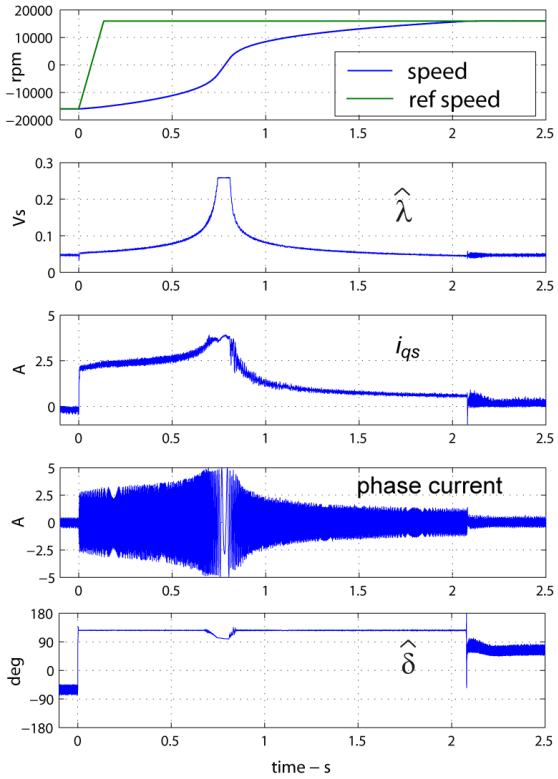

Figure 6. IPM motor speed reversal (–16000rpm÷16000rpm).

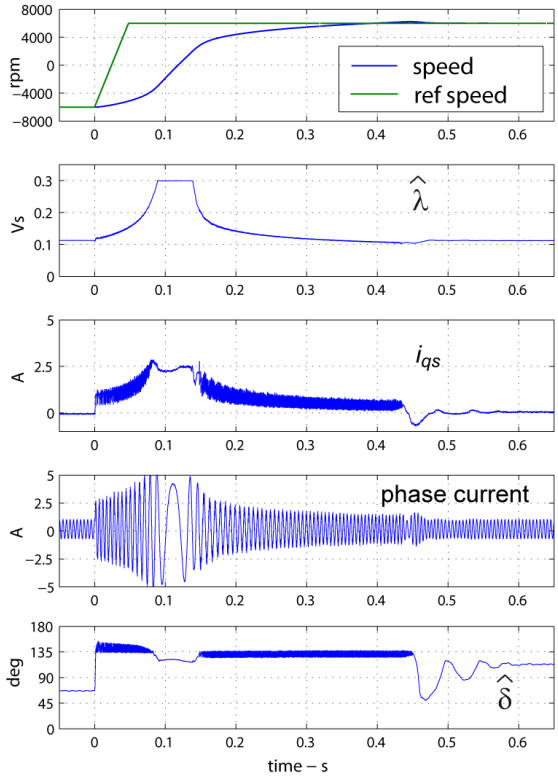

Figure 7. SyR motor speed reversal (–6000rpm÷6000rpm).

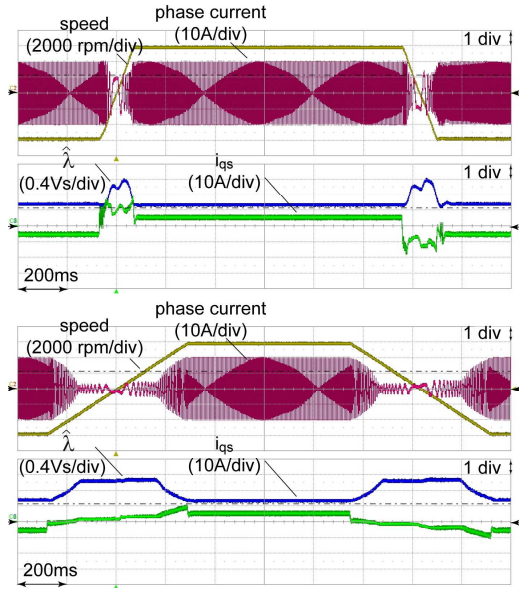

Figure 8. SPM motor speed reversal (–6000rpm÷6000rpm) with two different ramp slopes: 120000rpm/s (top) and 20000rpm/s (bottom).

C. *MTPV operation*

The trajectories of the flux vector in the *dq* rotor flux reference frame are shown for the IM, IPM and SyR cases, during the speed reversals described in the previous

subsection. The SPM motor has a limited flux weakening capability at rated current and has not been tested in MTPV operation, that would have required an 250% overload (i.e. a current greater than the characteristic current – see Table I). The flux trajectory of the IM motor is shown In Fig. 9, using an MTPV limitation at δ_{max} = 45°. The red and blue traces are superimposed and represent the deceleration and acceleration paths, respectively. As said, the noise in acceleration is due to the dc-link voltage ripple, since the flux amplitude reference is limited according to the current value of the dc-link, filtered by a first–order low-pass filter with cut-off frequency of 25 Hz. In Fig. 10-a the trajectories for the IPM motor have a poor quality due to the signals downsampling during the duration of the speed transient (2.5 s).

The load angle is limited at δ_{max} = 126° since the motor under test has a high saliency and a low per-unit PM flux.

In Fig. 10-b the trajectories for the SyR motor reveal the poor flux weakening capability of the drive (the rated flux is not so far from the MTPV angle). The load angle is limited at δ_{max} = 135°.

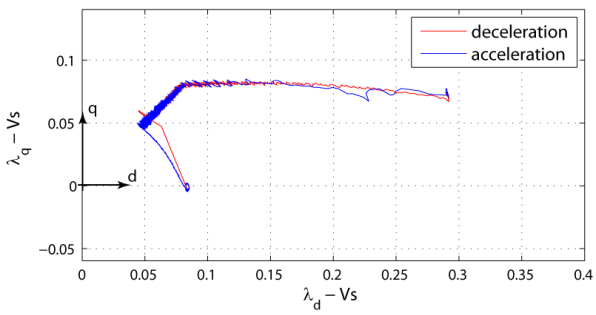

Figure 9. Trajectory of the IM observed flux in the during the speed reversal of Fig. 5. *d* and *q* are the observed rotor flux axes.

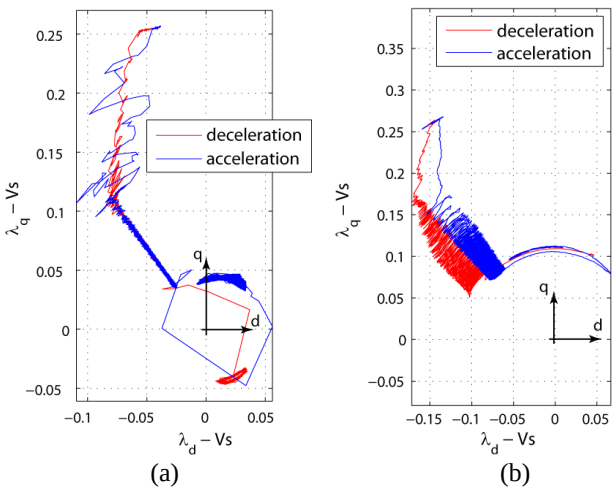

Figure 10. Trajectories of the observed flux in the during the speed reversals. a) IPM motor, refer to Fig. 6; b) SyR motor, refer to Fig. 7. *d* and *q* are the rotor axes given by the encoder.

D. *Low speed operation*

The load step response at low speed is presented for the IM and IPM motor cases in Figs. 11 and 12 respectively. Both the motor drives are speed controlled at 20 rpm and loaded by means of a torque-controlled DC motor. In both cases a 2.0 Nm torque step is applied and released, starting from and returning to no load conditions. The load step is within the current saturation limit in both cases. The speed responses are similar, in terms of peak transient speed error. With reference to the observed flux subplots, the IM flux reference (Fig. 11) is constant, independent of the reference torque, while the IPM motor flux reference is varied according to the torque set-point (Fig. 12). The low frequency component superimposed to i_{qs} in both tests is due to a torque disturbance introduced by the DC motor that depends on the mechanical speed.

VI. Conclusions

The proposed unified direct-flux vector control consists of a common control firmware that applies to four sinusoidal AC motor types. The only implementation difference is the motor model used in the stator flux observer for low-speed operation. Simplified or detuned motor models can produce steady-state torque estimation at low speed but no worse side-effects. The current and voltage limits are fully exploited by limiting the flux and torque current references with simple control laws that are independent of the motor parameters and valid also in case of a variable DC link. The control algorithm requires three PI regulators: two are for flux and i_{qs} current control and one is for load angle limitation at high speed.

The proposed scheme combines the advantages of the direct flux control along with only one current regulation channel for the torque-producing current component. In this way, both the flux-weakening and the current limitation are straightforward and easy to implement. The flux-current control is stable at high speed if the load angle limitation is used. Experimental results have been presented for all motors for heavy speed transients, demonstrating the feasibility of the proposed solutions.

References

[1] "The control techniques drives and controls handbook", W. Drury (Ed.), 2001. ISBN: 0-85296-793-4 & 978-0-85296-793-5.

[2] L. Harnefors, M. Jansson, R. Ottersen and K. Pietiläinen, "Unified Sensorless Vector Control of Synchronous and Induction Motors", IEEE Trans. Ind. Electron.,vol.50, No.1, February 2003, pp.153-160.

[3] I. Boldea, M.C. Paicu and Gh.-D. Andreescu, "Active Flux Concept for Motion-Sensorless Unified AC Drives", IEEE Trans. Power Electron., Vol.23, No.5, September 2008, pp. 2612-2618.

[4] C. Lascu, I. Boldea and F. Blaabjerg, "The Torque Vector Controlled (TVC) Universal AC Drive, Implementation Aspects, Conf. Rec. IEEE OPTIM 1998, vol.2, pp.369-374, 1998.

[5] G. Pellegrino, E. Armando and P. Guglielmi, "Direct Flux Field-Oriented Control of IPM drives with variable DC link in the Field-Weakening Region, IEEE Trans. Ind. Appl., Vol 45, Issue , September/October 2009, pp.1619-1627.

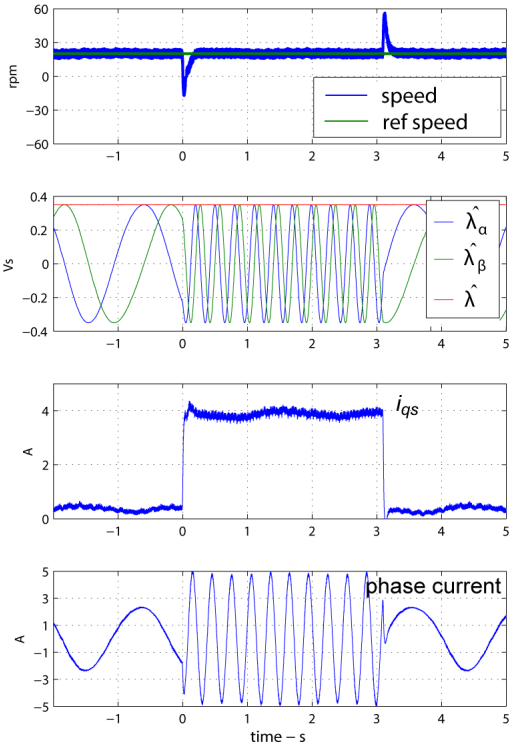

Figure 11. Load step response of the IM drive at 20 rpm. Load torque step is 2.0 Nm.

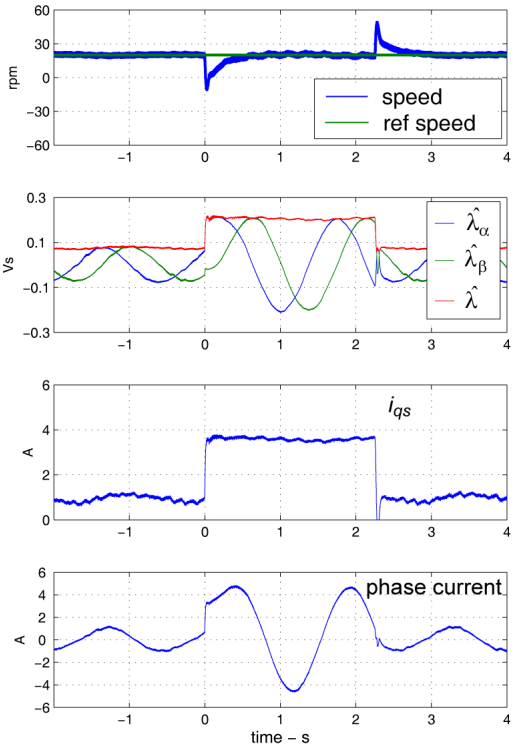

Figure 12. Load step response of the IPM motor drive at 20 rpm. Load torque step is 2 Nm.

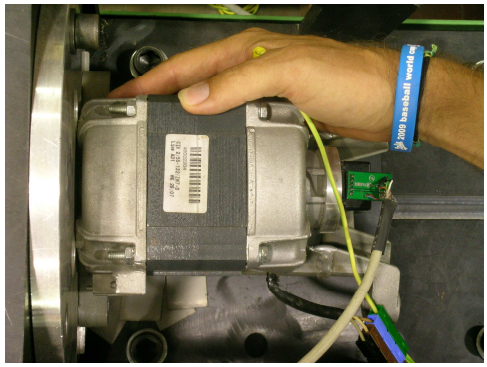

Figure 13. Picture of the IM under test.

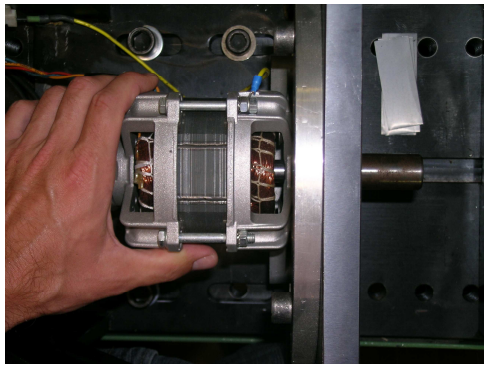

Figure 14. Picture of the IPM motor under test.

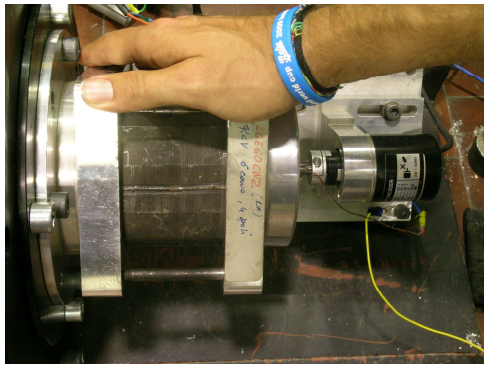

Figure 15. Picture of the SPM motor under test.

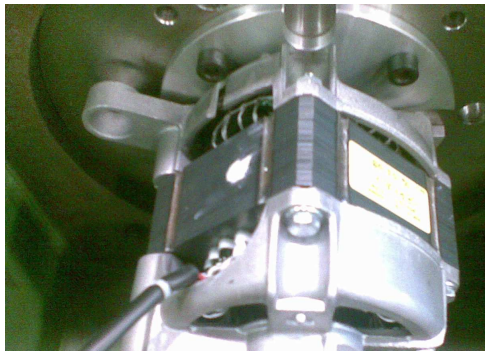

Figure 16. Picture of the SyR motor under test.

[6] R. Bojoi, P. Guglielmi and G. Pellegrino, “Sensorless Stator Field Oriented Control for Low Cost Induction Motor Drives with Wide Field Weakening Range” Conf. Rec. IEEE IAS 2008, pp. 1-7.

[7] P.L. Jensen and R.D. Lorenz, “A Physically Insightful Approach to the Design and Accuracy Assessment of Flux Observers for Field Oriented Induction Machine Drives”, IEEE Trans. on Ind. Applicat., Vol. 30, Issue 1, 1994, pp. 101-110.

[8] Holtz, J.; , “Sensorless control of induction motor drives,” Proceedings of the IEEE, vol.90, no.8, pp. 1359- 1394, Aug 2002

[9] N. Bianchi and S. Bolognani, “Magnetic Models of Saturated Interior Permanent Magnet Motors Based on Finite Element Analysis”, Conf. Rec. IEEE IAS 1998, Vol.1, pp. 27-34.

[10] A. Vagati, M. Pastorelli, F. Scapino and G. Franceschini, “Impact of Cross Saturation in Synchronous Reluctance Motors of the Transverse-Laminated Type”, IEEE Trans. Ind. Appl., Vol.36, No.4, July/August 2000, pp. 1039-1046.

[11] Xu, X.; de Doncker, R.; Novotny, D.W.; , “Stator flux orientation control of induction machines in the field weakening region,” Industry Applications Society Annual Meeting, 1988., Conference Record of the 1988 IEEE, vol., no., pp.437-443 vol.1, 2-7 Oct 1988

[12] Xu, X.; Novotny, D.W.; , "Implementation of direct stator flux orientation control on a versatile DSP based system," Industry Applications, IEEE Transactions on , vol.27, no.4, pp.694-700, Jul/Aug 1991

[13] W.L. Soong, T.J.E. Miller, “Field-weakening performance of brushless synchronous AC motor drives”, Electric Power Appl. , IEE Proceedings, Vol. 141, Issue 6, Nov. 1994, pp. 331-340.

[14] A.Vagati, M.Pastorelli, G.Franceschini, and V.Drogoreanu, “Digital Observer-Based Control of Synchronous Reluctance Motors,” in Conf. Rec of IEEE IAS 1997, Vol.1, pp. 629-636.

[15] K. Hurst, T. Habetler, G. Griva and F. Profumo, “Zero-Speed Tacholess IM Torque Control: Simply of Matter of Stator Voltage Integration”, IEEE Trans. on Ind. Appl., Vol. 34, Issue 4, July/August 1998, pp. 790-795.

APPENDIX

The motors under test are one commercial motor (IM) and two prototypes (IPM, SyR) for home appliances, while the last machine (SPM) is a prototype for industrial fans. The rating values of all motors are reported in Table I.

TABLE I - RATING VALUES OF THE FOUR MOTORS UNDER TEST

Motor type	IM	SPM	IPM	SyR
Rated torque (Nm)	2.6	4.4	1.4	0.73
Rated phase current (A pk)	4.2	5.6	2.8	2.4
Rated inverter current (A pk)	8	20	5	5
Rated line to line voltage (V pk)	270	270	270	270
Base speed (rpm)	3200	2700	3200	4000
Maximum speed (rpm)	16000	6000	16000	6000
Back emf at base speed (line to line – V pk)	/	250	70	/
Characteristic current (A pk)	/	50	2.0	/
Pole pairs	1	2	2	2
Stator slots	12	6	24	24
Stator diameter (mm)	110	107	95	95
Stack length (mm)	55	85	35	35

Gianmario Pellegrino (M'06) received the M.Sc. and Ph.D. degrees in electrical engineering from Politecnico di Torino, Turin, Italy, in 1998 and 2002, respectively.

He has been a Guest Researcher at Aalborg University, Denmark, in 2002. Since 2002 he has been with Politecnico di Torino, first as a Research Associate and then as an Assistant Professor, since 2007. He has been a visiting fellow at Nottingham University, UK, in 2010/2011. He is involved in research projects within the industry. He has more than 50 technical papers and one patent. His research areas are the electrical machines and drives, namely, the motor design and the digital control.

Dr. Pellegrino is an Associate Editor for the IEEE Transactions on Industry Applications. He is the corecipient of the IEEE-IAS EMC 3rd Paper Paper Award for ECCE 2009, the IEEE-IAS IDC 3rd Paper Paper Award for ECCE 2010 and the ICEM 2010 Best Paper Award.

Radu Iustin Bojoi (M'06, SM'10) received the M.Sc. degree in Electrical Engineering from the Technical University "Gh. Asachi" Iasi, Romania, in 1993, and the Ph.D. degree from Politecnico di Torino, Italy, in 2003.

Since 1994–1999 he was an Assistant Professor in the Department of Electrical Drives and Industrial Automation from Technical University of Iasi. In 2004 he joined the Department of Electrical Engineering of the Politecnico di Torino, where he is currently an Associate. Professor. His scientific interests regard the design and development of digital control systems in the fields of power electronics, high-performance electrical drives and power-conditioning systems. He has published more than 70 papers in international conferences and technical journals.

Paolo Guglielmi (M'07) received the M.Sc. degree in electronic engineering and the Ph.D. degree in electrical engineering from the Politecnico di Torino, Turin, Italy, in 1996 and 2001, respectively.

In 1997, he joined the Department of Electrical Engineering, Politecnico di Torino, where he became a Researcher in 2002. He has authored several papers published in technical journals and conference proceedings. His fields of interest include power electronics, high performance drives, and computer-aided design of electrical machines.